PROCEEDINGS OF THE INTERNATIONAL CONFERENCE
NANOMATERIALS: APPLICATIONS AND PROPERTIES
Vol. 4 No 2, 02NAESP06(4pp) (2015)

Detection of Structural Characteristics of Nanosized Sn_xS_y Film by the Modulation-polarization Spectroscopy of Plasmon Resonance

A.A. Vozny[1], M.O. Stetsenko[2,*], S.P. Rudenko[2], V.V. Kosyak[1], L.S. Maksimenko[2], A.S. Opanasyuk[1], B.K. Serdega[2]

[1] *Sumy State University, 2, Rymsky Korsakov Str., 40007 Sumy, Ukraine*
[2] *V. Lashkaryov Institute of Semiconductor Phisics, NAS of Ukraine, pr. Nauky 45, 03028 Kiev, Ukraine*

(Received 28 July 2015; published online 29 August 2015)

The present work deals with the study of the structural properties of nanosized SnS_2 films deposited by the close-spaced vacuum sublimation (CSVS) method. Surface morphology of the obtained films was determined by the scanning electron microscope (SEM-102E). Structural investigations of the films were performed with the Raman spectroscopy. The analysis of chemical composition of the layers was carried out by the scanning electron microscope by energy dispersive X-ray (EDS) spectroscopy. The structure features of Sn_xS_y films were investigated by the modulation-polarization spectroscopy (MPS) technique of surface plasmon resonance.

Keywords: Thin films, Sn_xS_y, Co-evaporation, Surface morphology, X-ray diffraction, Surface plasmon resonances, Modulation-polarization spectroscopy.

PACS numbers: 61.05.C –, 73.20.Mf, 61.72. – y

1. INTRODUCTION

The tin-sulfur system can form a variety of crystalline phases such as SnS, Sn_2S_3, SnS_2 with a different band gaps. A number of these compounds can be obtained by both p- and n-type conductivity. This allows creating solar cells (SC) with a heterojunction based on different phases of the same compound (e.g. n-SnS_2/*p*-SnS), which significantly simplifies their production and reduces cost [1]. Increasing of efficiency of SC needs optimization of structural characteristics of surface layers of Sn_xS_y as a component. Application of modulation-polarization spectroscopy (MPS) of surface plasmon resonance technique allows characterizing the structure of nanosized films by studying their polarization characteristics [2].

The interaction between electromagnetic radiation and metal, metal-dielectric and semiconductor films can manifest itself in a resonant excitation of surface plasmon polaritons (SPP) on infinite flat metal-dielectric surface or localized surface plasmons (LSP) on separated metal nanoparticles and between nanoparticles due to their dipole-dipole interactions [3]. Manifestation of surface plasmon resonance (SPR) in nanocomposite films takes place in presence of optical density in them or in a metal nanoparticles, such as gold nanoparticles in tin matrices of oxide or sulfide (SnO_2 and SnS_2) [4, 5]. The LSP excitations in Ag-SnS nanocomposite were studied in [6]. The materialisation of SPR in nanosized SnO_2 films without metal nanoparticles was shown in [7]. LSPR of anisotropic semiconductor nanocrystals was investigated in works [8, 9]. Therefore the questions about research of SPR phenomenon in nanosized Sn_xS_y films are important.

2. EXPERIMENTAL DETAILS

Sn_xS_y thin films were obtained on ultrasonically cleaned glass substrates in vacuum chamber under interstitial gas pressure not higher than $5 \cdot 10^{-3}$ Pa. Temperature of substrates was $T_s = 175$ °C. Film thickness was to 50 nm. The CSVS was used as growth method. This method allows to obtain films with small deviation from stoichiometry in conditions close to thermodynamic equilibrium. For this purpose a system for co-evaporation of sulfur and tin was created and approbated [10].

Surface morphology of the films was investigated by a scanning electron microscope (SEM-102E).

Thickness of the samples was studied using AFM (Digital Instrument's multimode scanning probe microscope (SPM) with"Nanoscope IIIa" controller).

The chemical composition of the films was estimated by X-ray radiation energy-dispersive analysis (EDS).

Structural analysis of the Sn_xS_y films was performed by Raman spectroscopy. The samples were studied by the Renishaw's Raman spectrometer at room temperature. The laser with a wavelength of 514 nm was used as excitation source.

The SPR is the most informative polarization effect in terms of properties of nanostructured films. Diagnostic of different SPR types with parameters of these resonances and information about optical parameters, morphological and structural features of nanomaterials was performed by measuring of polarization parameter as the polarization difference $\rho(\theta, \lambda)$.

Research setup [11] consisting of a goniometer connected to a monochromator allows to measure both the angular polarization characteristics of internal reflection parameters at various wavelengths λ and spectral characteristics at appropriate incident angles θ of radiation. The angular and spectral characteristics of the polarization difference $\rho(\theta, \lambda) = R_s^2 - R_p^2$ of the internal reflection coefficients at which polarization azimuths of radiation alternated between perpendicular and paral-

*StetsenkoMax@gmail.com

lel positions relative to the incident plane (*s*- and *p*-polarization, respectively) were investigated. If necessary, the angular and spectral dependences of $R_s^2(\lambda, \theta)$ and $R_p^2(\lambda, \theta)$ reflection coefficients separately were measured. Technical parameters of the measurement setup were as follows. A diffraction monochromator MDR-4 (with a halogen tube KGM-150 at the input and Franck-Ritter polarizer at the output) served as a source of spectral radiation in the wavelength range $\lambda = 0.4$-1 μm. A photoelastic polarization modulator [12] acted as dynamic phase plate with a modulation frequency of $f = 60$ kHz. The output radiation was directed at a photodetector PD (silicon photodiode). Detected signal was registered by a selective amplifier equipped with a phase-lock detector (lock-in-voltmeter) tuned to the modulation frequency. The variable component value was a magnitude of the difference of internal reflection coefficients of *s*- and *p*-polarizations. The resulting value is the polarization difference ($\rho(\lambda, \theta) = R_s^2 - R_p^2$).

3. RESULTS AND DISCUSSION

Figure 1 shows SEM image of Sn_xS_y films. It was determined that the films obtained at substrate temperature (T_s) 175 °C and thicknesses of 50 nm are polycrystalline and consist of platelet-shaped grains. The average grain size is 150 nm.

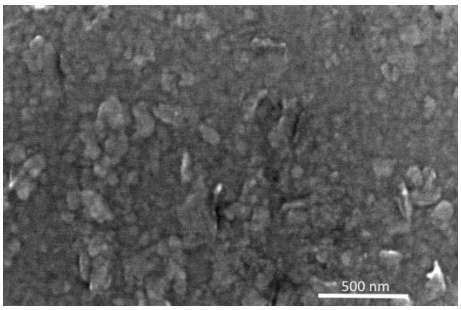

Fig. 1 – Plane-view SEM image of Sn_xS_y film obtained at $T_s = 175$ °C

The Raman scattering spectrum for the sample is shown in Fig. 2. As could be seen, the spectrum include strong peak at 315 cm^{-1} that corresponding to the A_{1g} mode of SnS_2 phase [13-15]. Weak Raman peak at 155 cm^{-1} is assigned to the Sn_2S_3 [16, 17]. The modes at 97, 224 and 288 cm^{-1} related to SnS phase were also detected [16, 18-20].

Figure 3 shows angular characteristics of polarization difference $\rho(\theta)$, reflection coefficients of *p*-polarized $R_p^2(\theta)$ and *s*-polarized $R_s^2(\theta)$ radiation. The sign of amplitude of $\rho(\theta)$ at various wavelength of radiation is changing due to different resonant contributions of *s*- and *p*-polarizations at surface plasmons excitations. These are confirmed by appropriate characteristics of $R_s^2(\theta)$ and $R_p^2(\theta)$ (Fig. 3b, c).

Figure 4 shows spectral characteristics of polarization difference $\rho(\lambda)$ at incident angles greater than the critical angle of total internal reflection ($\theta > \theta_{cr} = 43°$).

Asymmetrical contour in characteristics of $\rho(\lambda)$ can be caused by presence of two partially overlapping resonances in the films. On the one hand extremum in a short-wavelength range is caused by resonant excitation of localized surface plasmons (LSP) on rough surface of Sn_xS_y films. On the other hand extremum in a

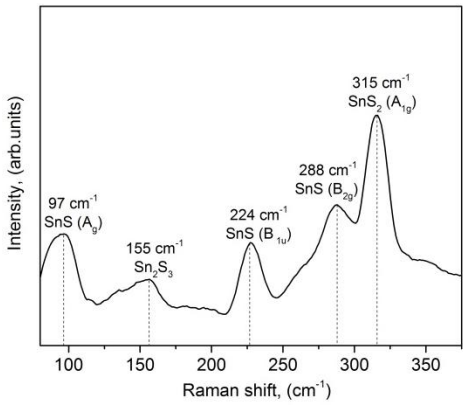

Fig. 2 – Raman scattering spectra of the sample

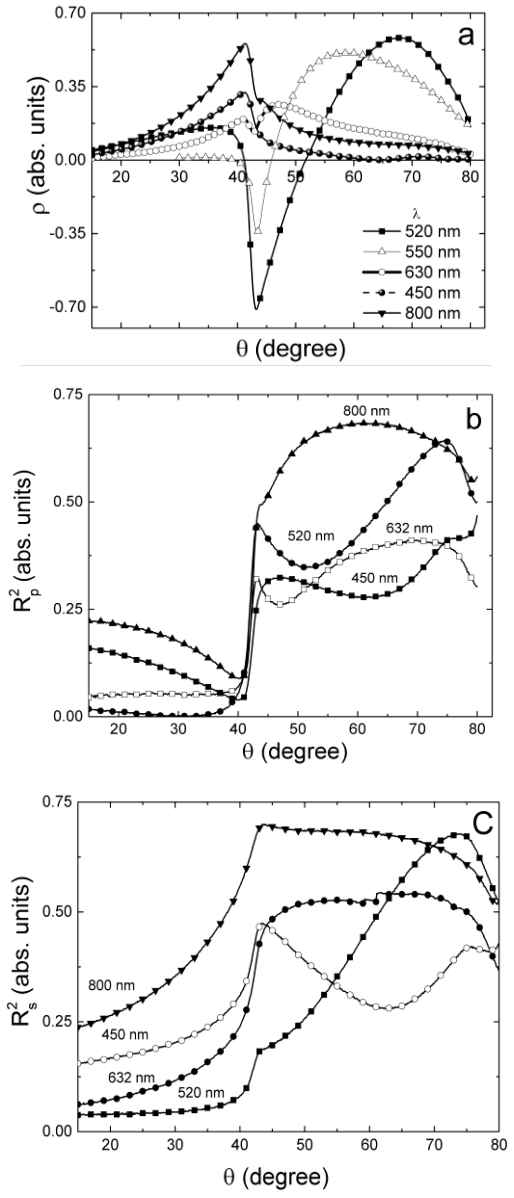

Fig. 3 – Angular dependencies: a) polarization difference; b) reflection coefficient of *p*-polarized; c) *s*-polarized light

long-wavelength range is caused by excitations of surface plasmon-polaritons (SPP) on continuous and homogeneous surface [21]. Phase-synchronous condition consists in coincidence of frequencies (ω) and wave vectors (k) of exciting radiation and surface plasmons and exists in the angle range of $\theta > \theta_{cr}$.

One can see that extrema of $\rho(\lambda)$ has a blue-shifts in the angle range of $43° < \theta < 60°$, which corresponding to LSP and SPP resonances: $\lambda_{LSP} = 527\text{-}477$ nm and $\lambda_{SPP} = 800\text{-}575$ nm, respectively. The minima in Figure 4(a) and 4(b) are caused by excitation of LSP in non-radiative and radiative modes, respectively. In Figure 4(b) minimum of $\rho(\lambda)$ at the angles less than the critical one $\theta < \theta_{cr}$ also has a slight blue-shift of $\lambda = 570\text{-}530$ nm.

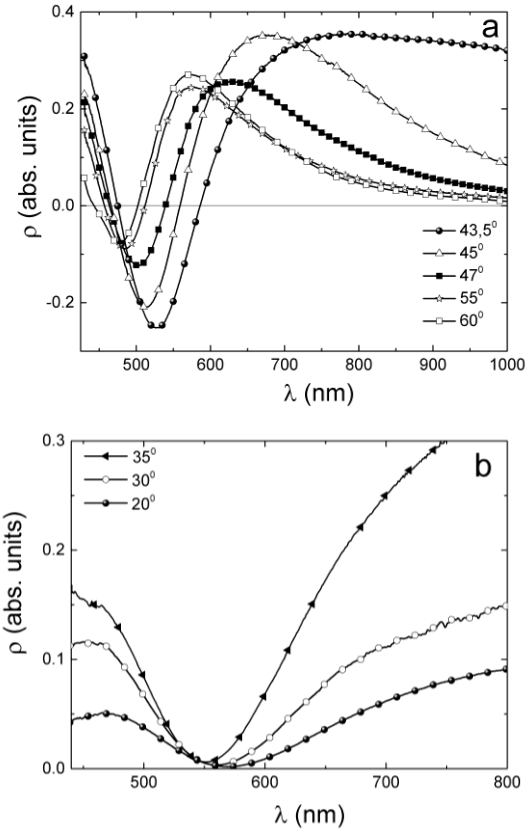

Fig. 4 – Spectral dependencies of the polarization difference in the angle range: a) 43.5°-60°, b) 20°-35°

The resonant excitations of LSP are determined by the extrema with negative values of $\rho(\lambda)$ due to greater interaction between films and s-polarization light and by the extrema with positive values of $\rho(\lambda)$ due to greater interaction between film and p-polarization light. Such curve features of $\rho(\lambda)$ are typical for nanosized films with a cluster structure.

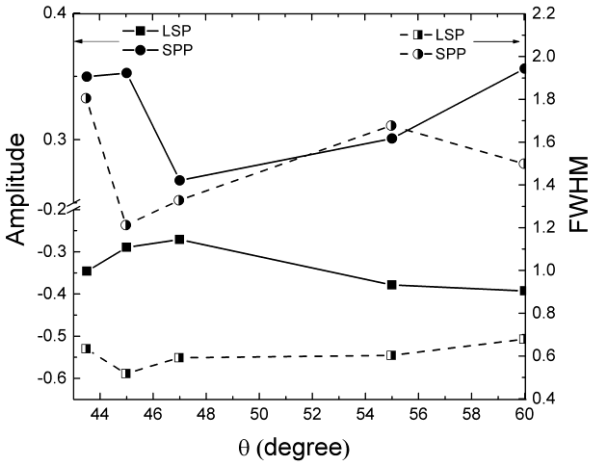

Fig. 5 – Angular dependencies of amplitude and FWHM of LSP and SPP resonances

Figure 5 shows dependencies of amplitude and FWHM (full width at half maximum) on the incident angle for LSP and SPP resonances. These results are obtained using procedure of decomposition of spectral dependencies into elementary components that are described by Gaussian function [22].

The FWHM parameter is responsible for the damping of resonance. It is shown that FWHM has a minimum at maximum amplitude both of LSP and SPP resonances. Moreover the minimum value of LSP corresponds to a maximum value of SPP in the angular amplitude dependencies of LPP and SPP resonances.

4. CONCLUSION

The surface morphology and phase composition of nanosized Sn_xS_y films with thickness of 50 nm obtained by CSVS method with a $T_s = 175$ °C were studied. For the first time two mechanisms of resonant interaction between radiation and electron subsystem of Sn_xS_y films with excitations of localized surface plasmons and surface plasmon-polaritons were shown in the angular and spectral characteristics of the polarization difference $\rho(\lambda, \theta)$ of internal reflection coefficients of s- and p-polarized radiation in the wide wavelength range of $\lambda = 400\text{-}1000$ nm.

With the help of diagnostic technique of modulation-polarization spectroscopy of surface plasmon resonance it was obtained that morphology surface of Sn_xS_y films has a inhomogeneous and continuous structure.

REFERENCES

1. A. Sanchez-Juareza, A. Ortiz, *J. Electrochem. Soc.* **147**, 3708 (2000).
2. L.J. Berezhinsky, L.S. Maksimenko, I.E. Matyash, S.P. Rudenko, B.K. Serdega, *Opt. Spectrosc.* **105**, 257 (2008).
3. S.A. Maier, *Plasmonics: fundamentals and applications* (Springer: 2007).
4. S. Singh, B.D. Gupta, *Meas. Sci. Technol.* **21**, 115202 (2010).
5. J. Li, Z. Yang, Y. Zhang, S. Yu, Q. Xu, Q. Qu, X. Hu. *Microchim. Acta* **179**, 265 (2012).
6. Priyal Jain, P. Arun, *J. Appl. Phys.* **115**, 204512 (2014).
7. V.S. Grinevich, L.M. Filevska, I.E. Matyash, L.S. Maximenko, O.N. Mischuk, S.P. Rudenko, B.K. Serdega, V.A. Smyntyna, B. Ulug, *Thin Solid Films* **522**, 452 (2012).
8. Su-Wen Hsu, Kathy On, Andrea R. Tao, *J. Am. Chem. Soc.* **133**, 19072 (2011).
9. Su-Wen Hsu, Charles Ngo, Andrea R. Tao, *Nano Lett.* **14**, 2372 (2014).
10. A.A. Voznyi, V.V. Kosyak, A.S. Opanasyuk, V.M. Kuznetsov, *Proc. NAP* **3** No1, 01NTF26 (2014).

11. L.J. Berezhinsky, L.S. Maksimenko, I.E. Matyash, S.P. Rudenko, B.K. Serdega, *Opt. Spectrosc.* **105**, 257 (2008).
12. S.N. Jasperson, S.E. Schnatterly, *Rev. Sci. Instrum.* **40**, 6 (1969).
13. M.G. Sousa, A.F. da Cunha, P.A. Fernandes, *J. Alloy. Compd.* **592**, 80 (2014).
14. I.P. Parkin, L.S. Price, T.G. Hibbert, K.C. Molloy, *J. Mater. Chem.* **11**, 1486 (2001).
15. V.G. Hadjiev, D. De, H.B. Peng, J. Manongdo, A.M. Guloy, *Phys. Rev. B* **87**, 104302 (2013).
16. Shuying Cheng, Gavin Conibeer, *Thin Solid Films* **520**, 837 (2011).
17. H.R. Chandrasekhar, D.G. Mead, *Phys. Rev. B* **19**, (1979).
18. H.R. Chandrasekhar, R.G. Humphreys, U. Zwick, M. Cardona, *Phys. Rev. B* **15**, 2177 (1977).
19. Louise S. Price, Ivan P. Parkin, Amanda M.E. Hardy, Robin J.H. Clark, *Chem. Mater.* **11**, 1792 (1999).
20. N.R. Mathews, C. Colın Garcıa, Ildefonso Z. Torres, *Mater. Sci. Semiconductor Proc.* **16**, 29 (2013).
21. E.B. Kaganovich, S.A. Kravchenko, L.S. Maksimenko, E.G. Manoilov, I.E. Matyash, O.N. Mishchuk, S.P. Rudenko, B.K. Serdega, *Opt. Spectrosc.* **110**, 513 (2011).
22. M.A. Stetsenko, *Optoelektronika i Poluprovodnikovaya Tekhnika* **49**, 93 (2014).